

A peer-reviewed version of this preprint was published in PeerJ on 12 June 2017.

[View the peer-reviewed version](https://peerj.com/articles/3438) (peerj.com/articles/3438), which is the preferred citable publication unless you specifically need to cite this preprint.

Chen CCM, Bourne DG, Drovandi CC, Mengersen K, Willis BL, Caley MJ, Sato Y. 2017. Modelling environmental drivers of black band disease outbreaks in populations of foliose corals in the genus *Montipora*. PeerJ 5:e3438 <https://doi.org/10.7717/peerj.3438>

Modelling environmental drivers of black band disease outbreaks in populations of foliose corals in the genus *Montipora*

Carla C.M Chen^{Corresp., 1,2}, David G Bourne^{1,3}, Chris Drovandi^{2,4}, Kerrie Mengersen^{2,4}, Bette L Willis^{3,5}, M. Julian Caley^{2,4}, Yui Sato¹

¹ Australian Institute of Marine Sciences, Townsville, QLD, Australia

² ARC Centre of Excellence for Mathematical & Statistical Frontiers, Queensland University of Technology, Brisbane, QLD, Australia

³ Marine Biology and Aquaculture, College of Science and Engineering, James Cook University, Townsville, QLD, Australia

⁴ School of Mathematical Sciences, Queensland University of Technology, Brisbane, QLD, Australia

⁵ ARC Centre of Excellence for Coral Reef Studies, James Cook University, Townsville, QLD, Australia

Corresponding Author: Carla C.M Chen

Email address: c.ewels@aims.gov.au

Seawater temperature anomalies associated with warming climate have been linked to increases in coral disease outbreaks that have contributed to coral reef declines globally. However, little is known about how seasonal scale variations in environmental factors influence disease dynamics at the level of individual coral colonies. In this study, we applied a multi-state Markov model (MSM) to investigate the dynamics of black band disease (BBD) developing from apparently healthy corals and/or a precursor-stage, termed 'cyanobacterial patches' (CP), in relation to seasonal variation in light and seawater temperature at two reef sites around Pelorus Island in the central sector of the Great Barrier Reef. The model predicted returning rate from BBD to Healthy in three months was approximately 57%, but 5.6% of BBD cases resulted in whole colony mortality. Healthy coral colonies were more susceptible to BBD during summer months when light levels were at their maxima and seawater temperatures were either rising or at their maxima. In contrast, CP mostly occurred during spring, when both light and seawater temperatures were rising. This suggests that environmental drivers for healthy coral colonies transitioning into a CP state are different from those driving transitions into BBD. Our model predicts that (1) the transition from healthy to CP state is best explained by rising light, (2) the transition between healthy to BBD occurs more frequently from early to late summer, (3) 20% of CP infected corals developed BBD, although light and temperature appeared to have limited impact on this state transition, and (4) the number of transitions from healthy to BBD differed significantly between the two study sites, potentially reflecting differences in localised wave action regimes.

1 Modelling environmental drivers of black band disease outbreaks in populations of foliose
2 corals in the genus *Montipora*

3

4 Carla C.M. Chen^{1,2*}, David G. Bourne^{1,3}, Chris Drovandi^{2,5}, Kerrie Mengersen^{2,5}, Bette
5 L. Willis^{3,4}, M. Julian Caley^{2,5} and Yui Sato¹

6

7 ¹Australian Institute of Marine Sciences, Townsville, QLD 4810, Australia

8 ²ARC Centre of Excellence for Mathematical & Statistical Frontiers (ACEMS), Queensland
9 University of Technology, Brisbane, QLD, 4001, Australia

10 ³Marine Biology and Aquaculture, College of Science and Engineering, James Cook University,
11 Townsville, QLD, 4811, Australia

12 ⁴ARC Centre of Excellence for Coral Reef Studies, James Cook University, Townsville 4811,
13 Australia

14 ⁵School of Mathematical Sciences, Queensland University of Technology, Brisbane, QLD 4001,
15 Australia

16

17

18 *Corresponding Author:

19 Carla C.M. Chen

20 Phone; 61 7 4753444

21 Fax; 61 7 47725852

22 E-mail: cewels@aims.gov.au

23

24 **Keywords:** Black Band Disease, Coral Disease, Environmental covariates, Multi-state Markov
25 model, transitional probability, Cyanobacterial patches, Seasonal variation

26 **Abstract**

27 Seawater temperature anomalies associated with warming climate have been linked to increases in
28 coral disease outbreaks that have contributed to coral reef declines globally. However, little is
29 known about how seasonal scale variations in environmental factors influence disease dynamics at
30 the level of individual coral colonies. In this study, we applied a multi-state Markov model (MSM)
31 to investigate the dynamics of black band disease (BBD) developing from apparently healthy
32 corals and/or a precursor-stage, termed 'cyanobacterial patches' (CP), in relation to seasonal
33 variation in light and seawater temperature at two reef sites around Pelorus Island in the central
34 sector of the Great Barrier Reef. The model predicted returning rate from BBD to Healthy in three
35 months was approximately 57%, but 5.6% of BBD cases resulted in whole colony mortality.
36 Healthy coral colonies were more susceptible to BBD during summer months when light levels
37 were at their maxima and seawater temperatures were either rising or at their maxima. In contrast,
38 CP mostly occurred during spring, when both light and seawater temperatures were rising. This
39 suggests that environmental drivers for healthy coral colonies transitioning into a CP state are
40 different from those driving transitions into BBD. Our model predicts that (1) the transition from
41 healthy to CP state is best explained by rising light, (2) the transition between healthy to BBD
42 occurs more frequently from early to late summer, (3) 20% of CP infected corals developed BBD,
43 although light and temperature appeared to have limited impact on this state transition, and (4) the
44 number of transitions from healthy to BBD differed significantly between the two study sites,
45 potentially reflecting differences in localised wave action regimes.

46

47 **Introduction**

48 Coral disease has contributed to localised declines in coral cover and changes in benthic communities
49 (Harvell et al. 2007; Weil et al. 2006). For example, in the US Virgin Islands, coral disease following a
50 mass beaching event in 2005 resulted in more than a 50% decline in coral cover, while in some areas of
51 the wider Caribbean, repeated outbreaks of white band disease resulted in benthic communities shifting
52 from coral to macroalgae dominated communities (Antonius 1981; Harvell et al. 2007). The impacts of
53 coral disease on reefs in other regions are not as extensively documented, although outbreaks have
54 been observed across the Indo-Pacific (Aronson & Precht 2001; Raymundo et al. 2005; Weil et al.
55 2012) and in some areas of Great Barrier Reef (Haapkylä et al. 2010; Page & Willis 2006; Sato et al.
56 2009; Willis et al. 2004).

57

58 Black band disease (BBD) presents as a virulent lesion that infects corals at reef locations worldwide,
59 including the Caribbean, Red Sea and Indo-Pacific (reviewed in Sato et al. (2016)). On the Great
60 Barrier Reef (GBR), BBD is also one of the most widespread coral diseases (Page & Willis 2006). It
61 appears as a darkly pigmented microbial mat occurring as a band at the interface between apparently
62 healthy coral tissue and freshly exposed skeleton. The BBD microbial mat consists of a polymicrobial
63 consortium, composed of a dominant cyanobacterium, sulfate-reducing and sulfide-oxidizing
64 bacteria, and other heterotopic microorganisms, which migrates across colonies killing the
65 underlying coral tissues (Miller & Richardson 2011; Richardson 2004; Sato et al. 2016). Linear
66 progression rates of the band of up to 2cm per day have been reported in the Caribbean (Kuta &
67 Richardson 1997), although typically it progresses more slowly (average: 0.3 cm/day;
68 (Sutherland et al. 2004). The abundance of BBD on coral reefs is generally low, with only 1 –
69 10% of colonies typically infected at any one time (Green & Bruckner 2000). Outbreaks can
70 occur however, such as observed in the Florida Keys National Marine Sanctuary in 1992, where

71 more than 50% of colonies within a population of *Montastraea annularis* were infected with the
72 disease (Kuta & Richardson 2002). At one study site on the GBR, BBD infections on
73 approximately 10% of colonies in an assemblage, resulted in an average loss of 40% of coral
74 tissue surface area, with colonies having a history of BBD infection being particularly
75 susceptible to re-infection (Sato et al. 2009). Therefore, even though BBD is potentially part of
76 the natural ecology of coral assemblages (Page & Willis 2006), an outbreak of BBD is capable
77 of reshaping a coral community (Bruckner & Bruckner 1997).

78 Environmental conditions, particularly seawater temperature and light irradiance, combined with
79 demographic factors, such as host diversity and density, have all been linked to the prevalence of
80 a number of different coral diseases (Harvell et al. 2009; Harvell et al. 2007). For BBD
81 specifically, changes in seawater temperature are thought to be a major environmental driver
82 (Antonius 1981; Edmunds 1991; Kuta & Richardson 2002; Rodriguez & Croquer 2008; Sato et
83 al. 2009). High seawater temperatures can influence the dynamics of coral diseases through
84 increased pathogen abundance and/or virulence, and/or increased host susceptibility as a result of
85 reduced immune capacity (Burge et al. 2014). However, reports that BBD occurs mostly on
86 corals in shallow habitats and is often absent from highly turbid waters suggest that spatial
87 variation in the occurrence of this disease may be governed by the response of the microbial
88 community associated with the lesion, particularly the dominant cyanobacterium, to different
89 light intensities (Cróquer & Weil 2008; Kuta & Richardson 2002; Page & Willis 2006).

90 During a two and a half year field monitoring study at a site in the central region of Australia's
91 Great Barrier Reef (GBR), cyanobacterium-dominated, green-brown lesions termed
92 cyanobacterial patches (CP) were identified as an early stage in the development of BBD
93 lesions (Sato et al. 2010). The microbial community of CP was dominated by a

94 cyanobacterium closely related to *Blennothrix* and *Trichodesmium spp.*, whereas the BBD
95 microbial community was predominately composed of an *Oscillatoria sp.*-related
96 cyanobacterium (Sato et al. 2010), currently classified as *Roseofilum reptotaenium* (Buerger et
97 al. 2016; Casamatta et al. 2012). During the monitoring period, approximately 19% of
98 colonies that presented with CP lesions (n=262 colonies) developed into visually characteristic
99 BBD lesions, although this percentage is likely to be an underestimate because of difficulties
100 accessing the sites during the monitoring period. Although the exact mechanism by which CP
101 transitions to BBD is still unknown, a pathogenesis model proposed by Sato et al. (2016)
102 suggests that light and temperature are the key drivers of this transition. A physiological
103 experiment using cyanobacterial cultures suggests that as light levels decrease from seasonal
104 maxima and seawater temperatures approach seasonal maxima, conditions became favourable
105 for the BBD-dominant cyanobacterium to outcompete the CP-associated cyanobacterium,
106 facilitating transitions within the microbial community (Glas et al. 2010; Sato et al. 2016).

107

108 Statistical methods for studying disease transitions are well established for many host-
109 pathogen interactions, and multi-state Markov models (MSMs) are particularly suitable for
110 describing processes whereby an individual progresses through different states in a disease
111 continuum and for exploring the roles of covariates in the process. For example, MSMs have
112 been widely used in studies of human diseases, such as HIV/AIDS (Aalen et al. 1997;
113 Gentleman et al. 1994; Mathieu et al. 2005), breast cancer (Meier-Hirmer & Schumacher
114 2013) and dementia (Joly et al. 2002), however the use of such models to describe coral
115 disease transitions is yet to be explored. Here, we apply a MSM to describe the development
116 of BBD in 355 coral colonies monitored on the inshore central GBR to examine how changes
117 in seasonal environmental conditions, in particular temperature and light, influence
118 transitions between healthy, CP and BBD states. Specifically, we (1) model the effects of

119 seasonal changes in temperature and light on progression of BBD lesions, (2) test conclusions
120 of the pathogenesis model proposed by Sato et al. (2016), and (3) provide a case study for
121 applying such model-based approaches to understand drivers of coral disease outbreaks.

122 **Materials and Methods**

123 *Data collection*

124 The dynamics of the coral diseases CP and BBD were monitored in two *Montipora* spp.-dominated
125 coral assemblages between September 2006 and January 2009, at sites in the central GBR located
126 at North-East (18°32.5'S, 146°30.0'E) and South-East (18°33.6'S, 146°30.1'E) Pelorus Island, as
127 detailed in Sato et al. (2009; 2010). Data from this comprehensive and intensive field monitoring
128 program were used to develop modelling approaches for assessing drivers of disease transitions
129 within coral populations. Both sites have limited exposure to terrestrial run-off but are exposed to
130 strong wave energy year-round caused by south-easterly trade winds. The site at NE Pelorus is
131 relatively more protected from waves than the SE Pelorus site. At each site, three replicate 10 m x
132 10 m permanent quadrants were haphazardly placed 5 to 10 m apart between 2.5 - 3.0 m depth. A
133 total of 355 coral colonies were individually tagged and photographed (239 colonies from SE
134 Pelorus; 116 colonies from NE Pelorus), and the state of each coral colony was recorded in repeated
135 surveys between September 2006 and January 2009 (see Sato et al. 2009, 2010 for full details). Due
136 to logistical limitations in accessing study sites caused by poor weather conditions, surveys were
137 done at irregular intervals (i.e., at one to three month intervals).

138 *Environmental Data*

139 Average daily seawater temperature and light irradiance levels were obtained from a weather
140 station operated by the Australian Institute of Marine Science located at nearby Orpheus
141 Island, approximately 8 km from the study sites. Seawater temperature was measured at 6 m
142 depth and light at the surface as photosynthetically active radiation (PAR, $\mu\text{mol photons m}^{-2}\text{s}^{-1}$).
143 As seawater temperature is a partial function of solar energy absorbed by the ocean, seasonal
144 patterns of light and seawater temperature are highly correlated (Supplemental S1). However,
145 seasonal patterns in seawater temperature lag behind seasonal light patterns, thus light levels
146 reach seasonal maxima/minima before seawater temperature. To incorporate the individual
147 effects of both light and seawater temperature and account for the lag between the two variables,
148 a new metric of environmental condition was developed by identifying four phases in annual
149 light and seawater temperature cycles: rising (\uparrow), maximum (M_{ax}), declining (\downarrow), and minimum
150 (M_{in}). To determine the seawater temperature phase at time t , a non-linear sinusoidal model was
151 first fitted to each of the datasets. The water temperature phase at time t was then determined by
152 the value of the slope of the non-linear function at point t , which is the first derivative of the
153 function. Even though a slope of zero is the theoretical turning point of functions (i.e. slope=0,
154 either at the maximum or the minimum; slope>0, rising phase; slope<0, decreasing phase), a
155 wider range of values was used here to reflect that water temperature often remains relatively
156 steady for a period before declining or increasing. Exploratory analysis suggested that a
157 threshold slope value of ≈ 0.7 best described the data. Therefore, when the slope was greater
158 than 0.7, temperature was deemed to be rising, and decreasing when the slope was less than -
159 0.7. Slopes between -0.7 and 0.7 were categorised as being either maxima or minima,
160 depending on the observed value (Figure 1).

161 A similar approach was used to derive light phases from daily average data. However, due to
162 large annual variation in light cycles (Figure 1b), different cosine functions were fitted to each

163 of the annual light cycles between July 2005 and July 2009. An annual light cycle was defined as
164 365 days starting from the lowest light period in July, and light data from July 2005 to July 2009
165 was used. Different threshold values were chosen for each annual cycle, based on the closest fit to
166 natural patterns in an exploratory analysis (i.e., 0.9 for 2006, 0.8 for 2007 and 2008, and 0.7 for
167 2009; Figure 1b).

168
169 The converted categorical variables of light and seawater temperature were combined to form a
170 single environmental metric using eight possible combinations (“ $M_{ax}\uparrow$ ”: light at maxima and
171 water temperature rising; “ $M_{ax}M_{ax}$ ”: both light and water temperature at maxima; “ $\downarrow M_{ax}$ ”: light
172 dropping and water temperature at maxima; “ $\downarrow\downarrow$ ”: both light and water temperature dropping;
173 “ $M_{in}\downarrow$ ”: light at minima and water temperature dropping; “ $M_{in}M_{in}$ ”: both light and water
174 temperature at minima; “ $\uparrow M_{in}$ ”: light rising and water temperature at minima; and “ $\uparrow\uparrow$ ”: both
175 light and water temperature rising). However, due to the logistics of assessing study sites in
176 poor weather conditions, only one observation for the “ $\uparrow M_{in}$ ”, “ $M_{in}\downarrow$ ” and “ $\downarrow M_{ax}$ ” phases were
177 available. Therefore, samples from these phases were combined with the nearest class (by
178 date), hence we use five possible phases of microclimatic condition, “ $M_{ax}M_{ax}$ ”, “ $M_{ax}\uparrow$ ”,
179 “ $\downarrow\downarrow$ ”, “ $\uparrow\uparrow$ ” and “ $M_{in}M_{in}$ ”.

180

181 *Application of a Multi-state model to explain CP-BBD disease transitions*

182 A multi-state Markov model (MSM) was used to model transitions between disease states
183 and refine environmental factors contributing to these transitions. This model is particularly
184 useful when observations are made at irregular time intervals, the exact transitional time is
185 unknown, subjects are recruited progressively, and survival times are right censored (e.g
186 death of some subjects is not reached by the end of study). In a MSM, the probability of
187 transition, i.e. moving from state r to state s , is governed by transitional intensity (q_{rs}), which

188 is the instantaneous risk of moving between two states (i.e r to s), and the time interval
189 between observations (t). When the effects of covariates are of interest, covariates are often
190 regressed on the transitional intensity using the proportional hazard model, which assumes
191 covariate effects are multiplicative, i.e $q_{rs}(x) = q_{rs}^{(0)} \exp(\beta_{rs}x)$ where $q_{rs}^{(0)}$ is the baseline
192 intensity and β_{rs} is the effective size of covariate x .

193

194 We used a time-homogeneous Markov model to explain the development of BBD lesions.
195 This model assumes the transition intensity is constant as a function of time, t , and
196 independent of the history of the process, but only dependent on the state that the coral
197 currently occupies. The time unit here is a month and a detailed description of the model is
198 available in Supplemental S2. In our study, BBD disease development is specified to have four
199 discrete states, including three transient states (Healthy, CP and BBD) and one absorbing
200 state (Dead) (Figure 2a). The healthy state was defined as a colony lacking any visual signs
201 of CP or BBD lesions when examined. This state included colonies that showed no disease
202 signs, although they may have had a lesion previously that has since disappeared. Death was
203 defined here as mortality of an entire coral colony. To investigate the effects of light and
204 water temperature conditions on the transition between healthy to diseased states, recovery,
205 and between two diseased states, covariates were applied to transitions between $H \rightarrow CP$,
206 $CP \rightarrow H$, $CP \rightarrow BBD$, $H \rightarrow BBD$ and $BBD \rightarrow H$. In addition to light and seawater temperature
207 phase, study sites (NE and SE Pelorus) and disease density were also included as covariates.
208 Disease density was defined as the number of infected coral colonies per 100 m^2 at the time
209 observed. Disease density was then categorized as: low (≤ 10), median (11-20) or high (≥ 21).
210

211 The *msm* package (Jackson 2007) in R was used for model fitting. Parameter estimation was
212 done using the Broyden-Fletcher-Goldfarb-Shanno (BFGS) algorithm. Likelihood ratio tests
213 were used to prevent overfitting, and the assumption of time-homogenous transition intensity

214 was examined using the method suggested by Kalbfleisch & Lawless (1985), which involves
215 fitting a time-dependent model, i.e. $q_{sr}(t) = q_{sr}e^{\lambda t}$ and testing if $\lambda = 0$.

216 Results

217 Disease states of 239 and 116 colonies of *Montipora sp.* from SE and NE Pelorus reefs,
218 respectively, were repeatedly recorded between September 2006 and January 2009 (17
219 observations per colony at SE Pelorus; 13 observations per colony at NE Pelorus). The median
220 duration between two observations was 1.67 months (range: 0.33 to 3.76 months)

221 The majority of corals within each assemblage remained in the healthy state between
222 observations, and 214 transitions from healthy to the CP state and 166 direct transitions from
223 healthy to the BBD state were also observed (Table 1). Eleven colonies that had no visual signs
224 of disease died during the study and the cause of their mortality could not be assigned. For corals
225 with CP, 160 transitioned back to the healthy state, 87 remained in the CP state and 43
226 progressed to BBD by the next survey. On only two occasions did corals in the CP state die
227 without a BBD lesion being observed, hence transitions from CP to death were omitted from the
228 subsequent MSM analyses. For corals displaying visual signs of BBD, 150 returned to a healthy
229 state, 116 remained in the BBD state, and 11 colonies died. The transition from BBD to CP was
230 observed 5 times; however, these represented new CP lesions elsewhere on the host coral after
231 the original BBD lesions had disappeared, indicating that these BBD lesions did not transition
232 back to the CP stage. Therefore, the transition from the BBD to CP state was also excluded from
233 the MSM analysis. The final disease model is shown in Figure 2b. The difference between the
234 log likelihood of the time-dependent and time-independent models was small (-2 log-likelihood
235 are 4354.405 and 4376.467). Therefore, the assumption of a time-independent MSM appears to
236 be justified.

237

238 The final model fit was significantly better than the model without covariates (LR= 392.546,
239 $p < 0.000$), but the likelihood ratio test demonstrated that not all covariates influenced the
240 transitions between all states. Site and light-temperature phases were important for transitions
241 from $H \rightarrow BBD$, however only light-temperature phases were important for the transition
242 intensities of $H \rightarrow CP$, $CP \rightarrow H$, and $BBD \rightarrow H$. Disease density did not significantly affect the
243 transition between $H \rightarrow CP$ or $H \rightarrow BBD$.

244

245 Transitions between healthy and disease states (CP or BBD) were affected by the light-
246 temperature phases. During the period when temperature was rising and light was either rising or
247 at its annual maximum (i.e. $\uparrow\uparrow$ or $M_{ax}\uparrow$), the transition intensity from $H \rightarrow CP$ was significantly
248 higher than the period when both light and temperature were in decline ($\downarrow\downarrow$; Table 2a); transition
249 intensities from $H \rightarrow CP$ were low and did not differ significantly among $\downarrow\downarrow$, $M_{in}M_{in}$ and $M_{ax}M_{ax}$
250 phases. This suggests that healthy coral colonies were more likely to be affected by CP during the
251 spring. In contrast, transitions from $H \rightarrow BBD$ occurred more frequently later in the summer
252 season. During the $M_{ax}\uparrow$ and $M_{ax}M_{ax}$ phases, healthy coral colonies were 5.21 and 3.5 times,
253 respectively, more likely to be affected by BBD than during the $\uparrow\uparrow$ phase (Table 2b). However,
254 there was little difference in the transition intensities between the $M_{in}M_{in}$, $\uparrow\uparrow$ and $\downarrow\downarrow$ phases.

255

256 The MSM results also showed strong spatial variation between the NE and SE Pelorus sites.
257 The estimated instantaneous transitions from $H \rightarrow BBD$ ($q_{H \rightarrow BBD}$) at NE Pelorus were 2.41
258 times (95% CI: 1.67-3.50) higher than at SE Pelorus. This suggests that healthy corals at NE
259 Pelorus more frequently contracted BBD than corals at the SE Pelorus site.

260

261 After accounting for the effects of covariates, the estimated baseline transition intensity, $q_{H \rightarrow CP}^{(0)}$, from
262 healthy into CP (H→CP) was slightly higher than transitioning from healthy to BBD ($q_{H \rightarrow BBD}^{(0)}$)
263 ($q_{H \rightarrow CP}^{(0)}$, mean 0.05, 95% CI: 0.040-0.065; $q_{H \rightarrow BBD}^{(0)}$, mean 0.019, 95% CI: 0.007-0.046, Table 3),
264 however this difference was not significant. This suggested that without the influence of site and
265 light-temperature phase, at any given time interval, the probability for H→CP is the same as
266 H→BBD.

267

268 Even though the transition from CP to healthy predominately occurred during the $M_{ax} \uparrow$, $M_{ax} M_{ax}$
269 and $\downarrow \downarrow$ phases (Table 2c), the effects of differing light-seawater temperature phases on this
270 transition was less clear. This was because a higher number of H→CP transitions occurred in the $\uparrow \uparrow$
271 phase (period immediately before $M_{ax} \uparrow$ phase) and the estimated mean sojourn time for CP (i.e. the
272 time remaining in the CP state) was 1.14 months (95% CI: 0.91-1.43). Therefore it is unclear if the
273 higher number of CP→H transitions was the result of light-temperature conditions or the
274 development of a host immune response to the disease. Similarly, we were unable to identify the
275 effect of light-seawater temperature phases on the transition from BBD→H, even though a high
276 number of transitions from BBD→H were observed during the $M_{ax} \uparrow$ and $M_{ax} M_{ax}$ phases (Table 2d),
277 as the estimated mean sojourn time for BBD was 2.67 months (95%CI: 0.98-7.34). Furthermore,
278 we found no significant difference in the sojourn times of BBD and CP among different light-
279 seawater temperature phases (ANOVA, $p=0.74$), suggesting that reverting to the healthy state
280 is likely due to the development of a host immune response to the disease.

281

282 After removing the covariate effect, coral colonies with CP were four times more likely to revert to a
283 healthy state than progress into the BBD state ($q_{CP \rightarrow H}^{(0)} = 0.68$ vs. $q_{CP \rightarrow BBD}^{(0)} 0.19$; Table 3). Once a
284 coral colony exhibited a BBD lesion, the estimated recovery rate (BBD→H) in three months was

285 approximately 53%. However, once a coral colony presented BBD, mortality was at least 30 times
286 higher than a healthy colony (BBD→dead v.s healthy→dead; Table 3).

287 Discussion

288

289 This study demonstrates the use of a multi-state analysis to understand the dynamics of a
290 BBD disease epizootic within a *Montipora* spp. coral assemblage and elucidate how the covariate
291 effects of light and temperature influence lesion state-transitions within individual colonies. Results
292 highlight that the combined effect of seasonal variation in light and seawater temperature is an
293 important driver for transitions of individual healthy *Montipora* sp. corals into either CP or BBD
294 disease states. The transition into each of the two disease states occurred mostly from spring to
295 summer, when light and seawater temperatures were rising or at their maxima ($\uparrow\uparrow$, $M_{ax}\uparrow$,
296 $M_{ax}M_{ax}$). The transition between $H\rightarrow CP$ occurred slightly earlier in the spring/summer season than
297 $H\rightarrow BBD$, suggesting that CP may act as a precursor to BBD infections in some cases, although CP
298 was more likely to heal ($CP\rightarrow H$) than transition to BBD, as found in a field study (Sato et al. 2010).
299 Overall, healthy corals were more likely to develop CP lesions than BBD lesions, and the
300 likelihood of CP developing was greater during spring when seawater temperatures and light
301 were increasing or at their maxima ($\uparrow\uparrow, M_{ax}\uparrow$), compared to autumn months when temperature and
302 light were declining ($\downarrow\downarrow$). The transition from healthy to CP subsided when light and temperature
303 both reached maxima (i.e. $M_{ax}M_{ax}$), suggesting that rising seawater temperatures are favourable
304 for the development of CP lesions but high temperatures above a certain threshold inhibited
305 development of CP lesions. This interpretation is supported by laboratory-based studies, which
306 found that high temperatures at summer maxima negatively affected growth of the dominant
307 cyanobacterium within CP lesions (Glas et al. 2010). Thus, lower growth rates of the dominant
308 cyanobacterium within CP lesions likely explains the lower probability of CP-development when

309 both light and temperature were at maxima. In contrast, evidence that growth of CP-derived
310 cyanobacteria in cultures was positively correlated with light intensity (Glas et al. 2010) explains
311 why the highest intensity of H→CP transitions occurred when light was at its maximum ($M_{ax}\uparrow$).

312

313 The transition intensity between healthy and BBD states peaked when light was at its maximum
314 and water temperature was rising or at its maximum ($M_{ax}\uparrow$, $M_{ax}M_{ax}$). The 3 to 5 times greater
315 probability of developing BBD during the $M_{ax}\uparrow$ and $M_{ax}M_{ax}$ phases than when both light and
316 temperature were rising ($\uparrow\uparrow$) suggests that certain light and potentially temperature thresholds
317 need to be reached before corals are susceptible to BBD. Previous field studies have showed
318 that BBD abundance is positively correlated with temperature and light intensity (Antonius
319 1981; Edmunds 1991; Kuta & Richardson 2002; Page & Willis 2006; Sato et al. 2009; Voss &
320 Richardson 2006; Weil & Cróquer 2008; Zvuloni et al. 2009). Culture-based studies of the
321 locally dominant cyanobacterium in BBD lesions show that its growth is enhanced at seasonal
322 temperature maxima, while light has little impact on its growth (Glas et al. 2010), corroborating
323 our field-based results. Aquarium-based experimental studies have also shown that both high
324 light and temperature can cause stress in coral hosts and are linked to an increase in BBD
325 virulence (Boyett et al. 2007; Sato et al. 2011). Furthermore, a recent metagenomic and
326 metatranscriptomic-based study on the *in-situ* development of BBD derived from CP showed that
327 increased cyanobacterial photosynthesis, which introduces fixed carbohydrates into the microbial
328 community, is a key to the development of BBD pathogenesis (Sato et al. in press). However, our
329 modelling approach did not detect a role for combined light and temperature variation to drive the
330 CP to BBD transition. However, this result is likely due to the small number of CP-infected
331 colonies developing into BBD (43 cases). Hence more observations are required to help elucidate
332 the impact of light and temperature on the transition between the two disease states.

333

334 In addition to seasonal variation, our results also suggest strong spatial variation in the
335 likelihood that colonies of *Montipora* transition from healthy to BBD states. Significantly
336 more transitions from healthy to BBD were recorded at the NE than the SE Pelorus site.
337 Considering that the distance between these two sites is less than 5km, the difference in BBD
338 susceptibility is likely to reflect localised environmental conditions, particularly differences
339 in local wave action. Reefs at SE Pelorus are typically exposed to high wave action, whereas
340 the NE Pelorus site is comparatively protected by a local headland. Constant surface
341 disturbances and turbidity caused by wave surge would reduce light intensity reaching the
342 reef substratum, thus light levels may regularly be lower at SE than at NE Pelorus,
343 accounting for differences in disease dynamics between the two sites.

344

345 The low explanatory power of BBD-infected coral density on the probability of BBD
346 development suggests that environmental factors are more important drivers of disease
347 occurrence than the density of potential pathogen sources. Evidence of spatial clumping of BBD-
348 infected corals in past monitoring studies led to the proposal that BBD spreads from infected
349 corals to new corals in a density-dependant manner (Bruckner et al. 1997; Page & Willis 2006;
350 Voss & Richardson 2006). In contrast, Edmunds (1991) reported that distributions of BBD-
351 infected corals were not clumped nor dependant on host-coral density, suggesting that BBD is not
352 highly contagious. The present study supports this latter hypothesis and suggests that the clumped
353 distribution of BBD may result from patchy distributions of other local environmental conditions
354 within reefs, such as bottom topology, light availability, and/or sedimentation rates.

355

356 MSM has commonly been used in medical research to understand the development of human
357 diseases. Our application of this approach to the dynamics of the virulent coral disease BBD,
358 specifically the effect of environmental covariates on the probability of transitioning between

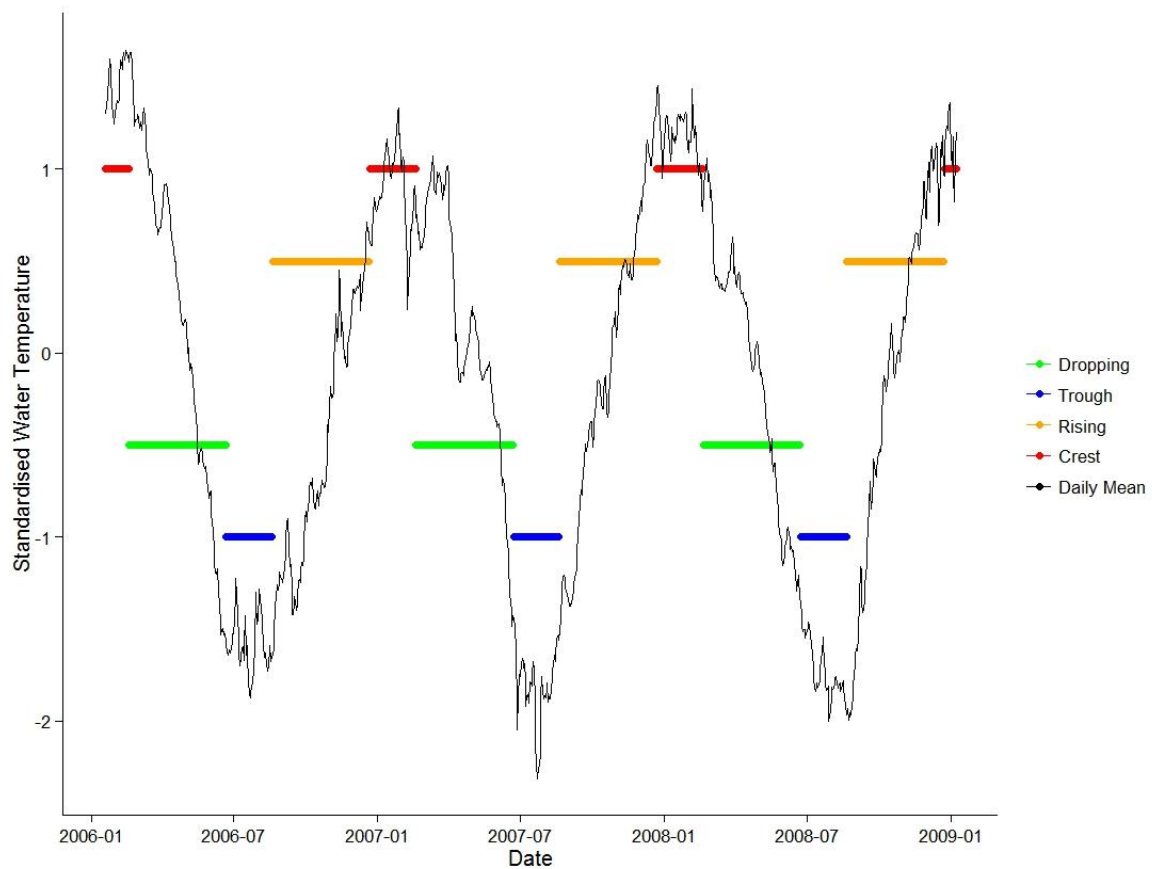
359 healthy and disease states in *Montipora spp.*, provides empirical support for the light-seawater
360 temperature hypothesis established in Sato et al. (2016). Although this study would have
361 benefited from a longer time series of observations made at shorter time-intervals, as well as
362 more comprehensive and localised measurements of environmental covariates at each study
363 site, it does provide a model-based framework for identifying the drivers of disease
364 transitions at fine spatial and temporal resolution. As the frequency of disease outbreaks is
365 predicted to increase with global changes in climate (Maynard et al. 2015), identifying the
366 drivers of finer spatial and temporal heterogeneity of disease outbreaks and spread is
367 becoming important, particularly for understanding the resilience of corals to climate change.
368 Our findings provide novel insights into disease dynamics at the scale of individual coral
369 colonies and identify environmental drivers leading to development of CP and BBD lesions
370 on corals.

371

372 **Acknowledgement**

373 Authors thank staff of James Cook University's Orpheus Island Research Station for their
374 logistic support. K. Chong-Seng, R. Littman, D. Loong, A. Lutz, T. Mannering, B. Olson, A.
375 Paley, A. Ridep-Morris, K. Schmidt, F. Seneca, P. Warner and K. Winters are also thanked
376 for their support in collection of specimens

377 |

378 **Figures and Tables**

379

380 **Figure 1a** Seasonal variation in seawater temperature at 6 m from January 2006 to January 2009, showing four
381 seasonal phases. Black line: daily mean temperature; blue lines: time period encompassing temperature minima;
382 green lines: period when temperature is decreasing; orange lines: period when light is rising; and red lines: period
383 when temperature at maxima.

384

385

386

387

388

389

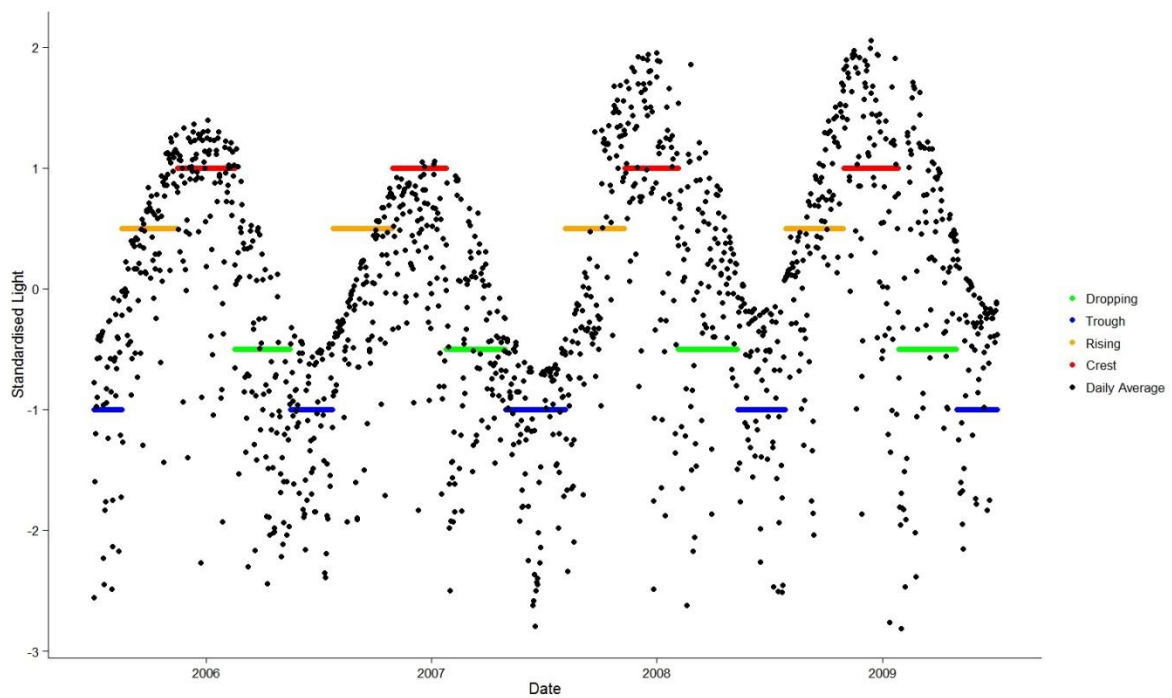
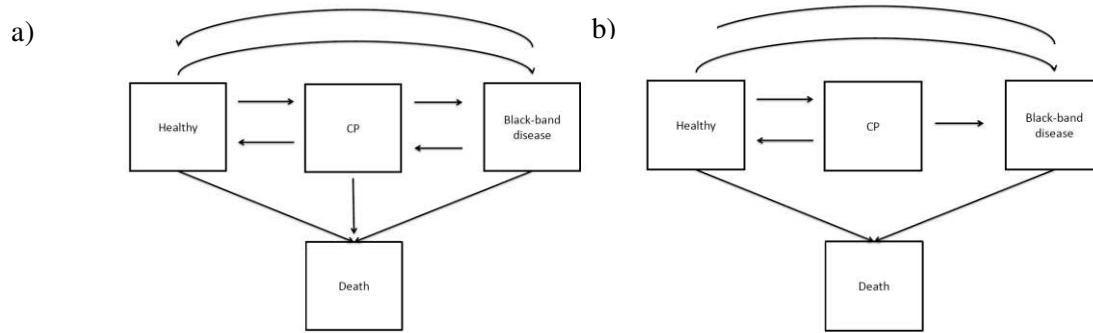


Figure 1b Seasonal variation in light from July 2006 to July 2009 and corresponding phases. Blue lines correspond to the light at trough, green lines are when light is at dropping phase, orange lines are when light is at rising phase and red lines are the light at crest.

390

391



392

393 **Figure 2 Modelling development of BBD lesions on the coral *Montipora* spp. Square boxes represent coral states and**
394 **arrows denote the direction of disease development. Except for the death states, transitions between transient states**
395 **are bi-directional. Figure a) is the initial disease model, and b) is the final model implemented in the analysis.**

396

397

398 **Table 1 Total number of state transitions occurring between 5030 pairs of consecutive observations from September**
 399 **2006 to January 2009.**

		To			
		Healthy	CP	BBD	Dead
From	Healthy	4065	214	166	11
	CP	160	87	43	2
	BBD	150	5	116	11

400

401

402 **Table 2: The effect of light-water temperature phase on the transition between two states. The light-water**
 403 **temperature is a categorical variable, thus the magnitude of phase effect is estimated using odds ratio. For example,**
 404 **the transition from healthy to CP was 2.85 higher during the $\uparrow\uparrow$ phase comparing to $\downarrow\downarrow$ phase. The two columns on**
 405 **the right are the estimated 95% confidence interval of the estimated odds ratio. $M_{in}M_{in}$ and $M_{ax}M_{ax}$ symbolize phases**
 406 **when both light and water temperature are at minima and maxima, respectively; $\uparrow\uparrow$ and $\downarrow\downarrow$ represent when both light**
 407 **and water temperature are rising and dropping, respectively; and $M_{ax}\uparrow$ represents when the light is at maxima while**
 408 **seawater temperatures are rising.**

Transition	Light-water temperature phase	Odds Ratio	Lower 95% CI	Upper 95% CI
a) Healthy \rightarrow CP	$M_{in}M_{in} / \downarrow\downarrow$	2.04	0.95	4.36
	$\uparrow\uparrow / \downarrow\downarrow$	2.85	1.35	6.02
	$M_{ax}\uparrow / \downarrow\downarrow$	3.56	1.66	7.62
	$M_{ax}M_{ax} / \downarrow\downarrow$	1.29	0.36	4.67
b) Healthy \rightarrow BBD	$M_{in}M_{in} / \uparrow\uparrow$	0.07	0.001	3.28
	$M_{ax}\uparrow / \uparrow\uparrow$	5.21	2.71	10.01
	$M_{ax}M_{ax} / \uparrow\uparrow$	3.50	1.46	8.39
	$\downarrow\downarrow / \uparrow\uparrow$	1.54	0.58	4.06
c) CP \rightarrow Healthy	$M_{in}M_{in} / \uparrow\uparrow$	1.37	0.68	2.80
	$M_{ax}\uparrow / \uparrow\uparrow$	3.36	1.92	5.89
	$M_{ax}M_{ax} / \uparrow\uparrow$	7.43	2.98	18.54
	$\downarrow\downarrow / \uparrow\uparrow$	3.67	1.39	9.91
d) BBD \rightarrow Healthy	$M_{in}M_{in} / \uparrow\uparrow$	1.54	0.77	3.08
	$M_{ax}\uparrow / \uparrow\uparrow$	8.27	4.37	15.67
	$M_{ax}M_{ax} / \uparrow\uparrow$	4.10	2.33	7.24
	$\downarrow\downarrow / \uparrow\uparrow$	0.01	0.000	31.96

409 **Table 3** Estimated baseline transitional intensity, $q_{rs}^{(0)}$ and 95% confidence interval between two included states.
 410 These are transitional intensities without the effect of covariates. For example, the transition from CP to BBD was
 411 significantly lower than the transition from CP to Healthy, as the mean estimates were 0.19 (95% CI: 0.132-0.274) and
 412 0.68 (95% CI: 0.51-0.905), respectively.

Transition	Mean estimates	Lower 95% CI	Upper 95% CI
Healthy→CP	0.051	0.04	0.065
Healthy→BBD	0.019	0.007	0.046
Healthy→Death	0.001	0.0003	0.003
CP→Healthy	0.680	0.51	0.905
CP→BBD	0.190	0.132	0.274
BBD→Healthy	0.301	0.086	1.04
BBD→Death	0.036	0.020	0.067

413

414

415

416

417

418

419

420

421

422

423 **References**

- 424 Aalen, O.O. et al., 1997. A Markov model for HIV disease progression including the effect of
425 HIV diagnosis and treatment: application to AIDS prediction in England and Wales.
426 *Statistics in medicine*, 16(19), pp.2191–2210.
- 427 Antonius, A., 1981. The “band” diseases in coral reefs. In *Proc 4th Int Coral Reef Symp.* pp. 7–
428 14.
- 429 Aronson, R.B. & Precht, W.F., 2001. White-band disease and the changing face of Caribbean
430 coral reefs. In *The Ecology and Etiology of Newly Emerging Marine Diseases*. Springer,
431 pp. 25–38.
- 432 Boyett, H.V., Bourne, D.G. & Willis, B.L., 2007. Elevated temperature and light enhance
433 progression and spread of black band disease on staghorn corals of the Great Barrier
434 Reef. *Marine Biology*, 151(5), pp.1711–1720.
- 435 Bruckner, A. & Bruckner, R., 1997. The persistence of black band disease in Jamaica: impact on
436 community structure. In *Proc 8th int coral Reef Symp.* pp. 601–606.
- 437 Bruckner, A.W., Bruckner, R.J. & Williams Jr, E.H., 1997. Spread of a black-band disease
438 epizootic through the coral reef system in St. Ann’s Bay, Jamaica. *Bulletin of Marine
439 Science*, 61(3), pp.919–928.
- 440 Buerger, P. et al., 2016. Genetic, morphological and growth characterisation of a new
441 *Roseofilum* strain (Oscillatoriales, Cyanobacteria) associated with coral black band
442 disease. *PeerJ*, 4, p.e2110.
- 443 Burge, C.A. et al., 2014. Climate change influences on marine infectious diseases: implications
444 for management and society. *Annual review of marine science*, 6, pp.249–277.
- 445 Casamatta, D. et al., 2012. Characterization of *Roseofilum reptotaenium* (Oscillatoriales,
446 Cyanobacteria) gen. et sp. nov. isolated from Caribbean black band disease. *Phycologia*,
447 51(5), pp.489–499.
- 448 Cróquer, A. & Weil, E., 2008. Spatial variability in distribution and prevalence of Caribbean
449 scleractinian coral and octocoral diseases-II Genera-level analysis. *Diseases of aquatic
450 organisms*, 83(3), p.209.
- 451 Edmunds, P.J., 1991. Extent and effect of black band disease on a Caribbean reef. *Coral Reefs*,
452 10(3), pp.161–165.
- 453 Gentleman, R. et al., 1994. Multi-state Markov models for analysing incomplete disease history
454 data with illustrations for hiv disease. *Statistics in medicine*, 13(8), pp.805–821.
- 455 Glas, M.S. et al., 2010. Cyanotoxins are not implicated in the etiology of coral black band
456 disease outbreaks on Pelorus Island, Great Barrier Reef. *FEMS microbiology ecology*,
457 73(1), pp.43–54.
- 458 Green, E.P. & Bruckner, A.W., 2000. The significance of coral disease epizootiology for coral
459 reef conservation. *Biological Conservation*, 96(3), pp.347–361.

- 460 Haapkylä, J. et al., 2010. Spatiotemporal patterns of coral disease prevalence on Heron Island,
461 Great Barrier Reef, Australia. *Coral Reefs*, 29(4), pp.1035–1045.
- 462 Harvell, D. et al., 2009. Climate change and wildlife diseases: when does the host matter the
463 most? *Ecology*, 90(4), pp.912–920.
- 464 Harvell, D. et al., 2007. Coral disease, environmental drivers, and the balance between coral and
465 microbial associates. *Oceanography*, 20, pp.172–195.
- 466 Jackson, C., 2007. Multi-state modelling with R: the msm package. *Cambridge, UK*.
- 467 Joly, P. et al., 2002. A penalized likelihood approach for an illness–death model with interval-
468 censored data: application to age-specific incidence of dementia. *Biostatistics*, 3(3),
469 pp.433–443.
- 470 Kalbfleisch, J.D. & Lawless, J.F., 1985. The Analysis of Panel Data Under a Markov
471 Assumption. *Journal of the American Statistical Association*, 80(392), pp.863–871.
472 Available at: <http://www.jstor.org/stable/2288545>.
- 473 Kuta, K. & Richardson, L., 1997. Black band disease and the fate of diseased coral colonies in
474 the Florida Keys. In *Proc 8th Int Coral Reef Symp.* pp. 575–578.
- 475 Kuta, K. & Richardson, L., 2002. Ecological aspects of black band disease of corals:
476 relationships between disease incidence and environmental factors. *Coral Reefs*, 21(4),
477 pp.393–398.
- 478 Mathieu, E. et al., 2005. Markov Modelling of Immunological and Virological States in HIV-1
479 Infected Patients. *Biometrical journal*, 47(6), pp.834–846.
- 480 Maynard, J. et al., 2015. Projections of climate conditions that increase coral disease
481 susceptibility and pathogen abundance and virulence. *Nature Climate Change*.
- 482 Meier-Hirmer, C. & Schumacher, M., 2013. Multi-state model for studying an intermediate
483 event using time-dependent covariates: application to breast cancer. *BMC medical
484 research methodology*, 13(1), p.80.
- 485 Meira-Machado, L.F. et al., 2008. Multi-state models for the analysis of time-to-event data.
486 *Statistical methods in medical research*.
- 487 Miller, A.W. & Richardson, L.L., 2011. A meta-analysis of 16S rRNA gene clone libraries from
488 the polymicrobial black band disease of corals. *FEMS microbiology ecology*, 75(2),
489 pp.231–241.
- 490 Page, C. & Willis, B., 2006. Distribution, host range and large-scale spatial variability in black
491 band disease prevalence on the Great Barrier Reef, Australia. *Diseases of aquatic
492 organisms*, 69, pp.41–51.
- 493 Raymundo, L.J. et al., 2005. Coral diseases on Philippine reefs: genus *Porites* is a dominant host.
494 *Diseases of aquatic organisms*, 64(3), pp.181–191.
- 495 Richardson, L.L., 2004. Black band disease. In *Coral health and disease*. Springer, pp. 325–336.

- 496 Rodriguez, S. & Croquer, A., 2008. Dynamics of black band disease in a *Diploria strigosa*
497 population subjected to annual upwelling on the northeastern coast of Venezuela. *Coral*
498 *Reefs*, 27(2), pp.381–388.
- 499 Sato, Y. et al., 2016. Integrated approach to understanding the onset and pathogenesis of black
500 band disease in corals. *Environmental microbiology*.
- 501 Sato, Y. et al. *In press*, Integrated genomics approach identifies the mechanism of black band
502 disease onset in corals. *The ISME journal*.
- 503 Sato, Y., Bourne, D. & Willis, B., 2011. Effects of temperature and light on the progression of
504 black band disease on the reef coral, *Montipora hispida*. *Coral Reefs*, 30(3), pp.753–761.
- 505 Sato, Y., Bourne, D.G. & Willis, B.L., 2009. Dynamics of seasonal outbreaks of black band
506 disease in an assemblage of *Montipora* species at Pelorus Island (Great Barrier Reef,
507 Australia). *Proceedings of the Royal Society of London B: Biological Sciences*,
508 276(1668), pp.2795–2803.
- 509 Sato, Y., Willis, B.L. & Bourne, D.G., 2010. Successional changes in bacterial communities
510 during the development of black band disease on the reef coral, *Montipora hispida*. *The*
511 *ISME journal*, 4(2), pp.203–214.
- 512 Sutherland, K.P., Porter, J.W. & Torres, C., 2004. Disease and immunity in Caribbean and Indo-
513 Pacific zooxanthellate corals. *Marine Ecology Progress Series*, 266, pp.273–302.
- 514 Voss, J.D. & Richardson, L.L., 2006. Coral diseases near Lee Stocking Island, Bahamas:
515 patterns and potential drivers. *Diseases of aquatic organisms*, 69(1), p.33.
- 516 Weil, E. et al., 2012. Extended geographic distribution of several Indo-Pacific coral reef
517 diseases. *Diseases of aquatic organisms*, 98(3), p.163.
- 518 Weil, E. & Croquer, A., 2008. Spatial variability in distribution and prevalence of Caribbean
519 scleractinian coral and octocoral diseases-I Community-level analysis. *Diseases of*
520 *aquatic organisms*, 83(3), p.195.
- 521 Weil, E., Smith, G. & Gil-Agudelo, D.L., 2006. Status and progress in coral reef disease
522 research. *Diseases of aquatic organisms*, 69(1), pp.1–7.
- 523 Willis, B.L., Page, C.A. & Dinsdale, E.A., 2004. Coral disease on the great barrier reef. In *Coral*
524 *health and disease*. Springer, pp. 69–104.
- 525 Zvuloni, A. et al., 2009. Spatio-temporal transmission patterns of black-band disease in a coral
526 community. *PLoS One*, 4(4), p.e4993.
- 527